Arginine Deprivation Affects mTORC1 Activation and Localization in Malignant Peripheral Nerve Sheath Tumors

A Senior Thesis Presented to
The Faculty of the Department of Molecular Biology,
Colorado College

By
Carly Merritt
Bachelor of Arts Degree in Molecular Biology
Submitted March 14th, 2018

Olivia Hatton

Dr. Olivia Hatton
Primary Thesis Advisor

Sara Hanson

Dr. Sara Hanson
Secondary Thesis Advisor

Carly Merritt

Abstract

Malignant peripheral nerve sheath tumors (MPNSTs) are rare, but highly aggressive sarcomas that often occur in patients with neurofibromatosis type I (NF1). Currently, surgical resection is the only treatment, but it is largely ineffective, resulting in a five-year survival rate between 20 and 50 percent. While MPNSTs are genetically and molecularly heterogeneous, mTOR is almost universally overexpressed in this cancer. Targeting the localization and activation of the mTOR complex mTORC1 within this subset of tumors may offer a strong potential treatment. As arginine is implicated in both mTORC1 localization and activation, modulating arginine levels may serve to regulate mTORC1. Importantly, arginine succinate dehydrogenase 1 (ASS1), an enzyme necessary for arginine synthesis, is suppressed in most sarcomas, causing cells to become reliant on extracellular arginine. Arginine deiminase reverts extracellular arginine to citrulline, effectively making arginine inaccessible by cells lacking ASS1. In this study, we set out to determine how arginine deprivation affects mTORC1 activation and localization and the potential impacts of mTORC1 on cellular metabolism. Using ADI-PEG20, a pegylated arginine deiminase drug, we deprived MPNST cells of arginine *in vitro*. To determine whether ADI-PEG20 could be effective at depriving cells of arginine, we first examined expression of ASS1 in MPNSTs and found heterogeneous expression among established MPNST cell lines. We found that depleting MPNSTs of arginine by ADI-PEG20 affects mTORC1 activation; however, this was independent of ASS1 expression, in contrast to our initial hypothesis. Because mTORC1 potentially interacts with hexokinase II (HK-II), a metabolic regulator, we examined the effect of arginine deprivation on mTORC1 binding to HK-II. mTORC bound HK-II independent of ASS1 expression. However, inactive mTORC1 preferentially bound to HK-II over active mTORC1. Finally, we explored MPNST metabolism, because previous studies have implicated mTORC1 interaction with HK-II in a switch from a glycolytic to OXPHOS phenotype. We found that MPNSTs favor an OXPHOS phenotype, an unusual metabolism in cancers. This association

between mTORC1, HK-II, arginine, and metabolism give preliminary data important in understanding this unique cancer's metabolism and methods of survival and may help to develop a treatment targeting MPNSTs.

Introduction

Malignant Peripheral Nerve Sheath Tumors (MPNSTs)

MPNSTs are a rare, but highly aggressive *Ras(H,N,K)*-driven soft tissue sarcoma with Schwannian origin, comprising ~2% of all sarcomas.[1] 50% of MPNSTs occur in conjunction with neurofibromatosis type I (NF1), while the other 50% of MPNSTs either occur sporadically or can be induced from radiation therapy.[1] Importantly, sporadic and NF1-associated MPNSTs are genetically indistinguishable, indicating there are no significant molecular differences between sporadic and NF1 associated MPNSTs.[2] Most NF1-associated tumors are benign plexiform neurofibromas which have the potential to transform into MPNSTs.[3] The pathway behind the transition from plexiform neurofibromas to MPNSTs is unclear, however it has been established that *NF1* mutations are not sufficient, as only 10% of NF1 patients develop MPNSTs.[1] MPNSTs are an especially dangerous cancer, with a five-year survival rate of only 20-50% that is largely due to the lack of treatments for MPNSTs. The current standard of therapy is surgical resection, which is only partially effective, and no chemotherapeutic treatments have demonstrated success.[4] Traditional chemotherapeutic agents (doxorubicin, cyclophosphamide, etoposide), as well as chemotherapies used in other sarcomas (sorafenib, imatinib, dasatinib) are minimally effective.[4, 5]

Traditional cancer therapies attack cells with a brute force cytotoxic approach, a strategy that often leads to serious side-effects and resistance. Understanding the molecular changes that result in cancer survival and proliferation offers a promising approach by exploiting weaknesses of specific cancers while minimizing damage to healthy cells.[6] MPNSTs can be characterized by Phosphatase and Tensin Homolog (PTEN) loss of function, Mitogen-activated protein kinase (MAPK) pathway and mammalian target of rapamycin (mTOR) upregulation, defects in apoptosis proteins and aurora kinases, and activation of the Wnt signaling pathway.[1] Mutations in *NF1*, seen in almost all NF1-associated MPNSTs and in around half of sporadic MPSNTs, are also often present.[1] NF1 is an autosomal dominant disorder resulting from a mutation or deletion of *NF1,* which encodes for the tumor suppressor Neurofibromin 1.[7] Neurofibromin 1 contains a GTPase-associated protein-related domain that inhibits the activity of Ras by catalyzing the conversion of of active Ras-GTP to inactive Ras-GDP. Without neurofibromin, Ras is hyperactive and the mammalian target of rapamycin (mTOR) is constitutively active, leading to tumorigenesis (Figure 1). mTOR pathway activation is ubiquitous in NF1-associated MPNSTs and it is also found in most sporadic MPNSTs.[8] Therefore, targeting the mTOR pathway seems to be a promising potential therapy. However, mTOR inhibitors like everolimus and rapamycin, while effective in lab, have had little success patients[9], so further research on the mTOR pathway and its inhibition are necessary.

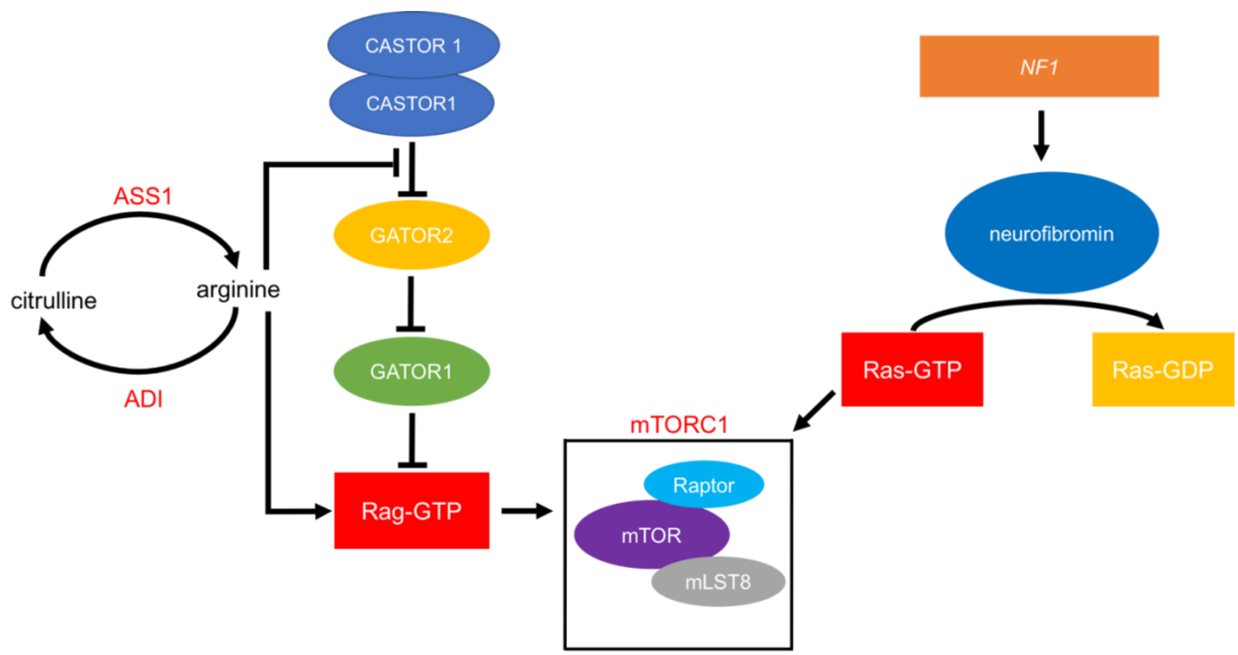

Figure 1. **mTORC1 is regulated by arginine and NF1 in MPNSTs**. ADI converts arginine to citrulline and ASS1 converts citrulline to arginine. Without arginine, CASTOR1 interacts with GATOR2 to inhibit mTORC1. Arginine binds to CASTOR1 to disrupt the CASTOR1-GATOR2 complex, resulting in the activation of Rag-GTP and mTORC1. NF1 codes for the tumor suppressor neurofibromin. Neurofibromin inhibits ras, controlling mTOR activity. Loss of NF1 function results in hyperactive mTOR.

mTOR and the mTORC1 Complex

Given the upregulation of mTOR that occurs with *NF1* mutations in MPNSTs, mTOR is commonly examined as a therapeutic target for these cancers. mTOR is a protein kinase important in regulating cell growth. It is a constituent of two distinct protein complexes - mTORC1 and mTORC2. mTORC1, activated by phosphorylation of Raptor, is composed of mTOR, Raptor, and mLST8 and regulates protein anabolism, nucleotide biosynthesis, lipogenesis, glycolysis, and autophagy (Figure 1).[10] mTORC2 is composed of mTOR, Rictor, SIN1, and mLST8 and regulates lipogenesis, glucose metabolism, the actin cytoskeleton, and apoptosis. While both mTORC1 and mTORC2 are upregulated in MPNSTs, the majority of previous attempts to target mTOR upregulation in MPNSTs have targeted the better characterized and more accessible mTORC1, and so we explored mTORC1 in our study.

Activity is not the only determinant of mTORC1 impact; subcellular localization plays a large part in mTORC1 functionality. In response to specific signals, mTORC1 has been found to localize to the lysosome, cytoplasm, endoplasmic reticulum, Golgi, nucleus, and mitochondria.[10] These localizations lead to different functions. For example, mTORC1 in the cytoplasm phosphorylates the translational inhibitor 4E-BP upon stimulation from growth factors to initiate translation.[11] Additionally, activation of Rag GTPase signaling has been shown to initiate mTORC1 translocation to the lysosome, where it phosphorylates multiple targets such as S6K, favoring protein synthesis or TFEB, preventing catabolic transcription.[12] One potential reason for the failure of targeted mTOR treatments in MPNSTs is that they have only targeted total mTORC1 activity, ignoring localization.

The amino acid arginine plays a role in both mTORC1 activity and localization. In one instance, arginine transported through SLC38A9 on the lysosomal membrane, disrupting a CASTOR1/GATOR2 heterodimer and thereby activating Rag GTPase (Figure 1).[13,14] This increased Rag GTPase signaling associated with arginine results in mTORC1 activation and localization to the lysosome.[14] When mTORC1 is localized to the lysosome, it phosphorylates TFEB, a transcription factor important in initiating autophagy.[15] Because arginine plays an important role in both mTORC1 localization and activation, and previous MPNST treatments have focused only on activation, targeting arginine-dependent mTORC1 localization and activation may be an effective alternate treatment for MPNSTs.

Arginine Deprivation as a Therapy

Arginine is a conditionally essential amino acid, meaning cells can usually produce enough endogenously to survive, but under certain conditions arginine must be supplied extracellularly. It plays an important role in the biosynthesis of proteins, and is especially relevant in cell division, wound healing, removing ammonia, immune function, and hormone release. In cells, it is the precursor to urea, creatine, polyamines, proline, glutamate, and nitric oxide.[16] In most cases, cells can produce arginine endogenously by converting citrulline to arginine with the enzyme arginosuccinate synthetase I (ASS1; Figure 1).[17] Most people create enough arginine endogenously via ASS1 that supplementation is unnecessary; however, growing children, pre-term babies, and adults with small intestine and kidney dysfunction require dietary supplementation.[18] Interestingly, ASS1 is not expressed in many cancers, making tumors reliant upon extracellular arginine for survival.[7] In fact, ~90% of sarcomas do not express ASS1 at levels considered high enough to provide the cell with sufficient arginine.[19]

Because MPNSTs are sarcomas and therefore probably do not express ASS1, they are likely dependent on extracellular arginine. This offers a target for slowing/stopping tumor growth, because in addition to arginine's relevance in protein biosynthesis, mTORC1 uses arginine for activation and localization. Arginine deiminase (ADI) is a hydrolase that converts arginine to citrulline.[17] A pegylated form of ADI, ADI-PEG20, has recently been developed as a therapeutic; when injected near the tumor site, it converts arginine in the tumor microenvironment to citrulline.[7] Because most sarcomas lack ASS1 necessary to convert citrulline back into arginine, this serves as an excellent technique to starve the tumor of arginine. One challenge with ADI-PEG20 is that some cells began to express ASS1 after prolonged use, counteracting the effects of the drug, meaning treatment must be balanced properly to avoid resistance.[19] Previous studies found that treatment of sarcomas with ADI-PEG20 alone promoted autophagy, while coupling ADI-PEG20 with traditional chemotherapy resulted in apoptosis and tumor shrinkage.[19] Interestingly, arginine deprivation has also been shown to affect cellular metabolism. One study has shown that treatment of glycolytic sarcomas with ADI-PEG20 downregulates aerobic glycolysis and increases oxidative phosphorylation (OXPHOS).[20]

Relationship between mTORC1, Hexokinase II, and metabolism

Metabolic reprogramming is an established hallmark of cancer with promising therapeutic targets. The most well-known metabolic phenotype of cancer is the Warburg effect, characterized by a shift in ATP generation through oxidative phosphorylation (OXPHOS) to aerobic glycolysis, the conversion of glucose to lactate under aerobic conditions.[21] While the Warburg effect is the most well-known cancer phenotype, it is not ubiquitous among cancers. Even in cancers that do exhibit a Warburgian phenotype, aerobic glycolysis accounts for ~60% of ATP generation, meaning even cancers exhibiting the Warburg effect still utilize OXPHOS.[22] In a single type of cancer, different tumors may have different metabolic phenotypes.[23]

Additionally, location within the tumor and timing also determines cellular metabolism. As the surrounding environment becomes more hypoxic, as in the center of a large tumor, glycolysis will be favored more because oxygen is unavailable, while cells on the outside of the tumor may favor aerobic glycolysis or OXPHOS.[24] This situational variability promotes the study of tumor metabolism on a more individual level, looking at cancer type, location, and tumor size to determine the ratio of aerobic glycolysis to OXPHOS. Understanding these metabolic differences allows for the development of specific metabolic treatments targeting each patient's tumors in the most effective way possible.

Hexokinase plays an important role in cellular metabolism where it phosphorylates glucose to produce glucose-6-phosphate (G-6-P) in the first step of glycolysis, the pentose phosphate pathway, and glyconeogenesis.[25] There are four isoforms of hexokinase, but hexokinase-II (HK-II) is the predominant isoform expressed in skeletal and cardiac muscles and in most cancers. Based on extra and intracellular signals, HK-II and mTORC1 can interact to shift cellular metabolism. During glucose deprivation, HK-II binds to and inhibits mTORC1, facilitating autophagy and conserving energy. However, under growth stimulating conditions, mTORC1 can activate HK-II and increase energy production.[25] This establishes a dual role for HK-II as both producing and conserving energy. In many cancer cells exhibiting the Warburg effect, HK-II binds to voltage-dependent ion channel 1 (VDAC1), an outer mitochondrial membrane protein.[26] This mitochondrial binding is important in coupling glycolysis and OXPHOS because it prevents G-6-P from inhibiting HK-II's function, and allows for preferential access to ATP [27], so HK-II upregulation is a major contributor to the aerobic glycolysis phenotype seen in many cancers.[26]

A recent study found evidence that mTORC1 may inhibit mitochondrial HK-II activity under stress conditions[28]. Researchers found that irradiating colon cancer and glioma resulted in a shift of mTORC1 localization from the cytosol to the mitochondria, where it bound to HK-II. This occurred without changing the overall amount of mTORC1 in the cell. This switch in localization and binding with HK-II corresponded with a switch from aerobic glycolysis to OXPHOS, indicating cancer cells can re-program their metabolism for survival and that the mTORC1 and HK-II interaction may play a part in metabolic shifts (Figure 2).[28] Incorporating metabolism into the study of mTORC1 in MPNSTs could provide information that may be useful in developing treatments.

In this study, we found that arginine deprivation inconsistently affects mTORC1 activation, localization, and interaction with HK-II in MPNSTs in a manner independent of ASS1 expression. We also found that MPNSTs favor an OXPHOS metabolism, unusual in cancer cells, and potentially related to the interaction between mTORC1 and HK-II. We first determined which MPNSTs expressed ASS1 and then treated established MPNST cell lines with ADI-PEG20. We examined activation by the phosphorylation of the mTORC1 component Raptor and localization by examining the interaction between mTORC1 and HK-II. Because of arginine, mTORC1, and HK-II's effect on metabolism, we also explored MPNST metabolism using cellular respiration assays.

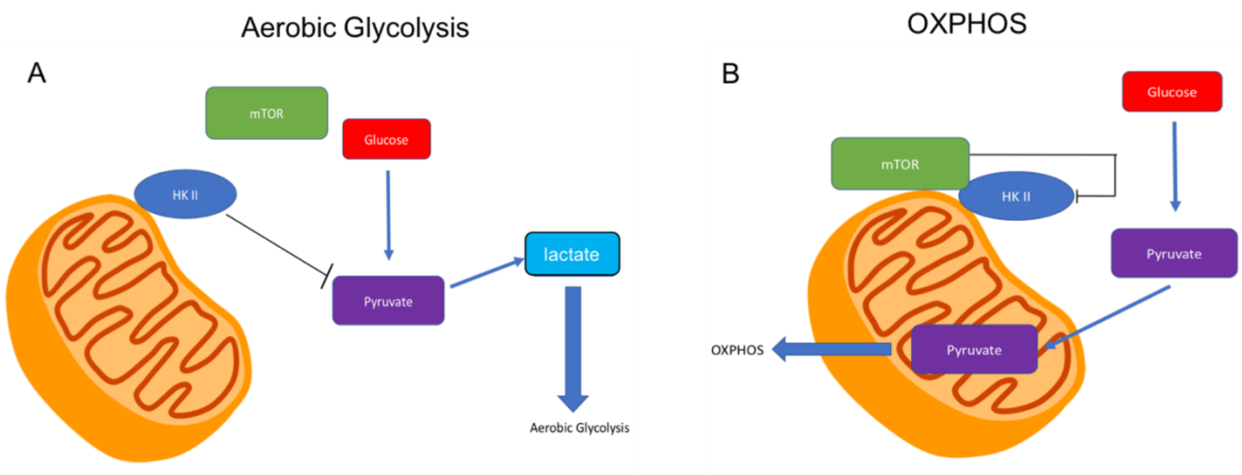

Figure 2. Proposed model for mTORC1-hexokinase II interaction. A) In aerobic glycolysis, hexokinase II is bound to the mitochondrial surface, allowing the cell to employ a glycolytic metabolism by blocking pyruvate's entry to the mitochondria. During this time, mTOR is localized in the cytosol. B) During OXPHOS, mTOR binds to the mitochondria, inhibiting hexokinase II (HKII), allowing pyruvate to enter the mitochondria, leading to OXPHOS metabolism.

Results

MPNST cell lines have mixed expression of ASS1

To determine how arginine alters mTORC1 activity and localization in MPNSTs, we first determined if MPSNTs express ASS1, the enzyme necessary for converting citrulline to arginine. A previous study performed on primary tumors in 45 of the most common sarcoma subtypes showed that ASS1 was absent in ~90% of tumors.[19] Notably, immunohistochemical results indicated that only 6 out of 75 MPNST tumors studied expressed ASS1.[19] To determine if this trend continued in established MPNST cell lines, Western blot analysis was carried out on immortalized human Schwann cells (iHSC), plexiform neurofibromas, and MPNSTs. Examining ASS1 expression in plexiform neurofibromas and iHSCs indicates ASS1 expression over the development of MPNSTs. Levels of ASS1 were compared to MG63, an osteosarcoma with high expression of ASS1.[19] Lines 26T and 724 are sporadic, while S462, 1488, MP642, ST03, and 96.2 are associated with NF1. In freshly isolated cellular lysates, the MPNST cell lines 26T, 1488, and 96.2 express ASS1 at similar to elevated levels relative to MG63, while 724, S462, MP642, and ST03 showed no ASS1 expression (Figure 3). It is of note that ASS1 expression faded in 1488 and 96.2 cells after freeze-thaw, completely disappearing on the second freeze-thaw cycle (data not shown), indicating that ASS1 expression may be unstable in these tumors. Neither iHSCs nor any of the plexiform neurofibroma cell lines express ASS1, indicating that ASS1 expression may be triggered in the transition from benign to malignant tumors. These data indicate that some MPNSTs express ASS1, although their iHSC and plexiform neurofibroma precursors do not. Because some cells lack ASS1 expression, these variants of MPNST tumors may be susceptible to treatment by arginine deprivation. We were curious to see if arginine deprivation may affect a dysregulated aspect of MPNSTs, mTORC1.

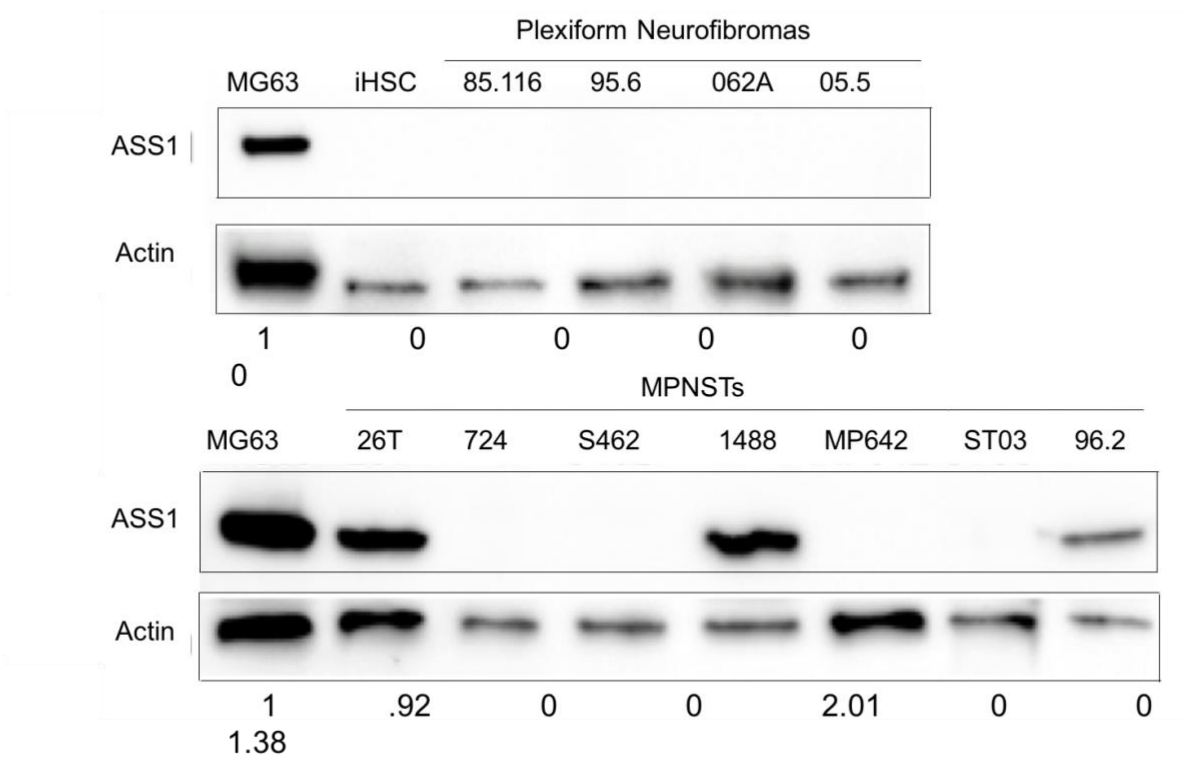

Figure 3. MPNSTs have mixed ASS1 expression. A Western blot for ASS1 was performed on 40 μg of immortalized human Schwann cells (iHSC), plexiform neurofibromas, and MPNSTs. Blots were also probed for β-actin as a loading control. MG63, an osteosarcoma, served as a positive control for ASS1 expression. This blot is representative of n=2 experiments. Densitometry calculated using ImageJ. ASS1 and β-actin normalized to MG63 and numbers represent ASS1 normalized to β-actin.

Arginine Deprivation Affects mTORC1 Activity and Expression in MPNSTs

To determine if arginine starvation through ADI-PEG20 treatment affects mTORC1 activation and expression in MPNSTs, Western blot analysis for phosphorylated and total Raptor was carried out on human Schwann cells (HSCs) and MPNSTs that either expressed or did not express ASS1. Primary HSCs have not undergone the genetic alterations required for immortality, and thus are a better model for protein expression and activation. HSC (ASS1$^-$) and 96.2 (ASS1$^+$) lines showed an increase in the ratio of P-Raptor to Raptor upon treatment with ADI-PEG20 compared to untreated cells, indicating an increase in active mTORC1 (Figure 4). ST03 (ASS1$^-$), 26T (ASS1$^+$), and 1488 (ASS1$^+$) lines showed a decrease in the ratio of P-Raptor to Raptor upon treatment with ADI-PEG20, indicating a decrease in active mTORC1 (Figure 4). Additionally, treatment with ADI-PEG20 reduced Raptor, and thus mTORC1, expression in HSC (ASS1$^-$), 26T, 1488, and 96.2 (all ASS1$^+$) compared to untreated cells, while ST03 (ASS1$^-$) treated with ADI-PEG20 increased Raptor expression compared to untreated cells (Figure 4, densitometry not shown). These data indicate that arginine deprivation can either increase or decrease mTORC1 expression and activation, and this effect is not dependent on ASS1 expression.

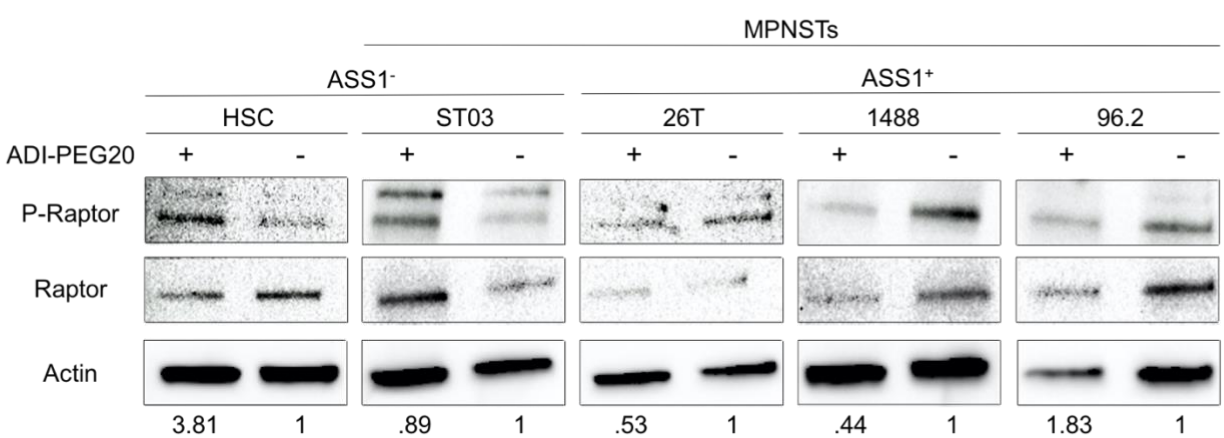

Figure 4. Arginine deprivation through ADI-PEG20 treatment affects mTORC1 activation. A Western blot was performed on 40 μg of human Schwann cells (HSC) and MPNSTs treated as indicated with 1 μg/mL of ADI-PEG20. Cross reacting bands present in some P-Raptor blots. Blots were also probed for β-actin as a loading control. This blot is representative of n=1 experiments. Densitometry calculated using ImageJ. P-Raptor and Raptor normalized to β-actin and numbers represent ratio of P-Raptor to Raptor in treated compared to untreated cells.

Inactive mTORC1 preferentially binds to hexokinase II in MPNSTs

Previous studies have shown that mTORC1 and HK-II interact, so we next examined if arginine deprivation altered the physical interaction between mTORC1 and HK-II. To determine how arginine affects mTORC1 binding to HK-II, co-immunoprecipitation was performed for active and inactive mTORC1 and HK-II. In cell lines where arginine deprivation decreased mTORC1 activation (STO3 and 26T), the ratio of P-Raptor to Raptor bound to HK-II increased upon treatment with ADI-PEG20 (Figure 5). HSC and 1488 did not show binding of P-Raptor to HK-II with ADI-PEG20 treatment (Figure 5). While both ADI-PEG20 treated and untreated 96.2 showed binding to HK-II, the treated had an absence of Raptor, so densitometry could not be carried out (Figure 5). HSC and 96.2 both showed a decrease in mTORC1 activity after arginine deprivation, and these (in addition to 1488) showed (apparently) increased HK-II binding. These data indicate that lines with increased mTORC1 activity upon arginine deprivation have decreased HK-II binding upon arginine deprivation (HSC, 96.2), and lines with decreased mTORC1 activity upon arginine deprivation have increased HK-II binding upon arginine deprivation (ST03, 26T), with 1488 being the exception. This pattern indicates that inactive mTORC1 may preferentially bind to HK-II in MPNSTs, compared to active mTORC1.

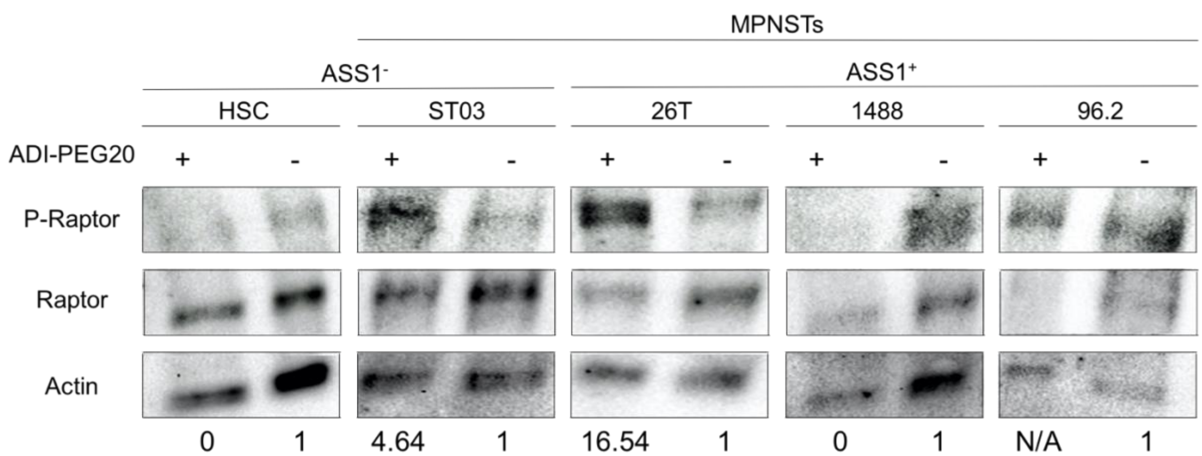

Figure 5. Active and inactive mTORC1 bind to hexokinase II. Human Schwann cells (HSC) and MPNST lysates were treated as indicated with 1 µg/mL of ADI-PEG20 for 24 hours. After immunoprecipitation for Hexokinase II, a Western blot for P-Raptor and Raptor was performed. Whole lysate was loaded and blotted for β-actin as a loading control. This blot is representative of n=1 experiments. Densitometry calculated using ImageJ. P-Raptor and Raptor normalized to β-actin and numbers represent ratio of P-Raptor to Raptor in treated compared to untreated cells.

A change in binding is often associated with a change in cellular location; for example, binding to Rheb localizes mTORC1 to the lysosome.[9] Therefore, we explored the interaction between mTORC1 and HK-II in the context of cellular location. In preliminary studies, we examined the localization of the mTORC1-HK-II interaction after a time course of arginine deprivation. Immunofluorescent chemistry showed that both HK-II and P-Raptor localize to the cytoplasm (Figure 6, Supplementary Figures 1 and 2). Puncta of red and green indicate co-localization of HK-II and P-Raptor. In both HSC and MP642 lines, there were very few puncta in untreated cells (Figure 6, top left panels), indicating low levels of P-Raptor and HK-II co-localization. However, after ADI-PEG20 treatment for 4 and 6 hours, many more puncta became visible (Figure 6, top right and bottom left panels), indicating that ADI-PEG20 treatment increases P-Raptor and HK-II co-localization. Interestingly, after 24 hours of ADI-PEG20 treatment, the number of puncta decreases, which matches data from the co-IP (Figure 6, bottom right panels). Together, these data support the co-localization of mTORC1 and HK-II in MPSNTs. They also show arginine deprivation can alter mTORC1 localization; however, these effects may be transient. With no correlation between ASS1 expression in cell lines and the increase or decrease of mTORC1 co-localization with HK-II, these data confirm that the effects of arginine deprivation are independent of ASS1 expression.

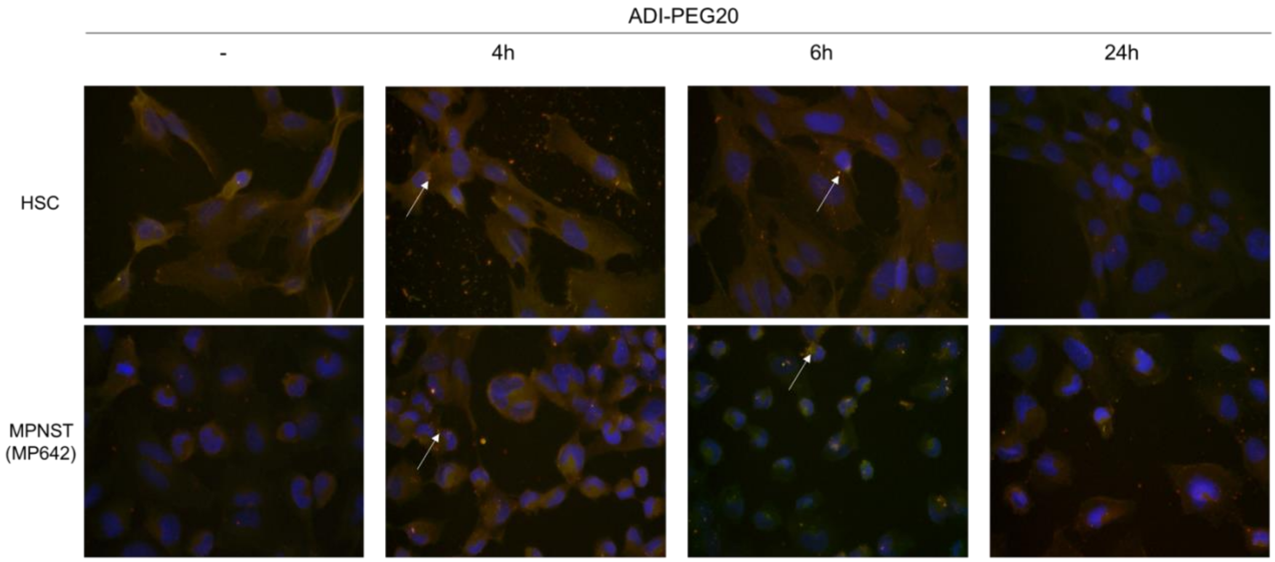

Figure 6. mTORC1 co-localizes with hexokinase II. Schwann cells (HSC) and MPNST cells (MP642) were fixed and labeled after 1µg/mL of ADI-PEG20 treatment for 0, 4, 6, and 24 hours. Nuclei were labeled with DAPI (blue). Phosphorylated Raptor was labeled with AlexaFluor (red). Hexokinase II was labeled with FITC (green). White arrows point to puncta, indicating co-localization of Hexokinase II and P-Raptor. This is representative of n=1 experiments.

OXPHOS is the preferred energy source over aerobic glycolysis in MPNST

A previous study showed that the interaction of mTORC1 and HK-II at the mitochondria led to an OXPHOS metabolism in other cancers[28], and we saw evidence of mTORC1 and HK-II interaction in MPNSTs. Additionally, arginine deprivation has been shown to affect the metabolism of sarcomas.[20] These metabolic implications sparked preliminary experiments on MPNST metabolism. To determine the metabolic phenotype of MPNSTs, Seahorse analysis for the base oxygen consumption rate (OCR), which indicates OXPHOS, and extracellular acidification rate (ECAR), which indicates aerobic glycolysis, was performed on immortalized human Schwann cells (iHSC), and MPNST cell lines. Seahorse technology functions by detecting dissolved oxygen (OCR) and free protons (ECAR) in extremely small volumes of cellular suspension to examine cellular respiration. All cells showed significantly higher rates of OCR than ECAR, indicating OXPHOS is preferred over aerobic glycolysis (Figure 7A). To determine if the high rates of OCR corresponded to energy production, Seahorse analysis was used to determine the percent of OCR coupled to ATP synthesis. Showing that OCR is coupled to ATP synthesis shows that the OCR corresponds to energy production, and not another cellular action like fat storage. All cell lines showed at least 70% OCR coupled to ATP synthesis (Figure 7B), indicating at least 70% of ATP is generated by OXPHOS versus aerobic glycolysis or other pathways, providing further evidence that MPNSTs utilize an OXPHOS metabolism.

To confirm these results, Western blots were used to determine levels of phosphorylated lactate dehydrogenase (P-LDH) and phosphorylated pyruvate dehydrogenase (P-PDH). P-LDH catalyzes the transformation of pyruvate to lactate, leading to aerobic glycolysis. P-PDH inhibits the transformation of pyruvate to Acetyl CoA, inhibiting OXPHOS. 26T, 724, S462, MP642, and ST03 lines showed expression of P-LDH an indicator of aerobic glycolysis. iHSC, 1488, and 96.2 lines did not express P-LDH, indicating OXPHOS (Figure 7C). iHSC, 26T, ST03, and 96.3 all showed extremely low levels of P-PDH expression, indicating OXHPOS. 724 showed no P-PDH expression, indicating OXPHOS, and 1488 showed level of P-PDH expression comparable to the positive control SKLMS1, indicating aerobic glycolysis (Figure 7C). The data strongly indicates that iHSC and 96.2 favor OXPHOS, while there is variability in other cell lines.

Finally, to determine if MPNSTs can compensate for OXPHOS loss, ATP synthase was inhibited with oligomycin and levels of ATP, OCR, and ECAR were measured. When iHSCs were treated with oligomycin, OCR levels decreased, but ECAR and ATP levels increased (Figure 7D, top left), indicating iHSCs can compensate for OXPHOS loss with aerobic glycolysis. When MPNSTs (724, 26T, S462, and ST88) were treated with oligomycin, ECAR levels increased (Figure 7D), indicating MPNSTs can switch to aerobic glycolysis under OXPHOS inhibition. However, OXPHOS inhibition resulted in a decrease in ATP (Figure 7D), indicating aerobic glycolysis cannot compensate for the loss of OXPHOS regarding ATP production. These data combine to indicate that OXPHOS is the preferred energy source over glycolysis in MPNSTs, and that they cannot energetically compensate if OXPHOS is inhibited, implying OXPHOS may be a good target for treatment.

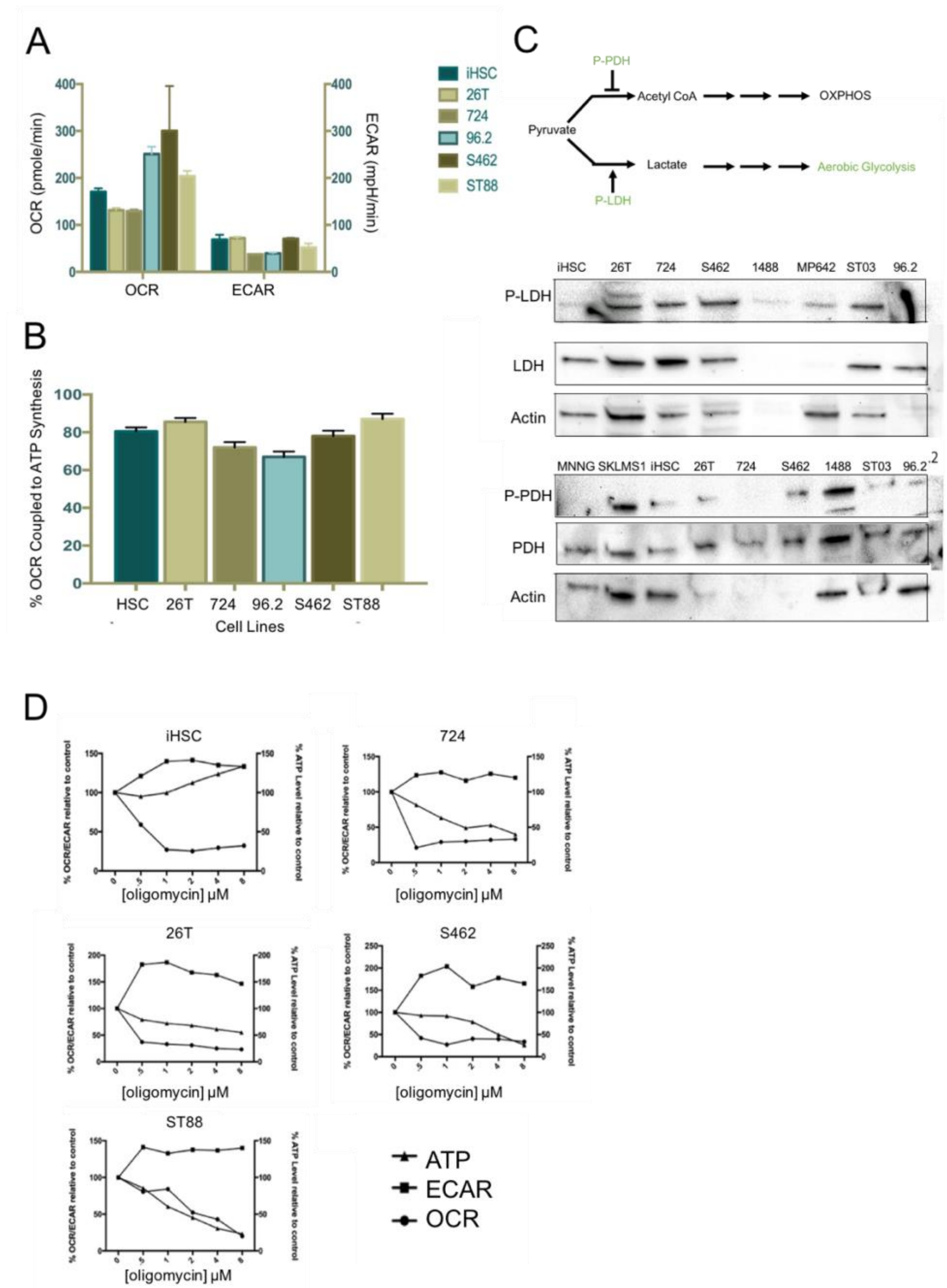

Figure 7. OXPHOS is the preferred energy source over glycolysis in MPNST. A) Base levels of oxygen consumption rate (OCR) and extracellular acidification rate (ECAR) were measured using Seahorse analysis in MPSNT and immortalized human Schwann cell (iHSC) cell lines. OCR corresponds to OXPHOS and ECAR corresponds to aerobic glycolysis. B) Percentage of ATP coupled to oxidative metabolism was measured using Seahorse analysis. C) P-PDH inhibits pyruvate forming Acetyl CoA, leading to aerobic glycolysis. P-LDH inhibits pyruvate forming lactate, leading to OXPHOS. 40 μg of immortalized human Schwann cells (iHSC), human Schwann cells (HSC), MPNSTs (26T, 724, 1488, ST03, 96.2, MP642), osteosarcoma (MNNG), and leiomyosarcoma (SKLMS1) protein were loaded and probed for phosphorylated and total LDHA and PDH1. MNNG served as a negative control for P-PDH, SKLMS1 served as a positive control for P-PDH. D) ATP synthase was inhibited with oligomycin and levels of ATP, OCR, and ECAR were measured using Seahorse analysis.

Discussion

In this study, we examined how arginine deprivation affects mTORC1 localization and activation in MPNSTs as well as the metabolism of MPNSTs that may be associated with mTORC1-HK-II localization. To determine whether arginine deprivation could have an effect on mTORC1 activation and localization, we first examined expression of ASS1 in MPNSTs and found mixed results. Depleting MPNSTs of arginine by ADI-PEG20 affected mTORC1, however this was independent of ASS1 expression, in contrast to our initial hypothesis. Because mTORC1 can interact with hexokinase II (HK-II), we examined the effect of arginine deprivation on mTORC1 binding to HK-II. Again, there were mixed results independent of ASS1 expression. We also found that inactive mTORC1 preferentially bound to HK-II over active mTORC1. We explored MPNST metabolism, as targeted metabolic treatments have been shown to be highly effective in treatment and because previous studies have implicated mTORC1 interaction with HK-II in a switch from a glycolytic to OXPHOS phenotype. We found that MPNSTs favor an OXPHOS phenotype, an unusual metabolism in cancers. Overall, these results indicate that arginine deprivation influences mTORC1 activation, localization, and binding to HK-II in a manner independent of ASS1 expression, and that MPNSTs have a unique OXPHOS metabolism which may be associated with the interaction between mTORC1 and HK-II.

We first found that some MPNSTs appear to gain ASS1 expression upon switching to malignancy. Western blots for ASS1 indicated that no plexiform neurofibromas express ASS1, however two of the MPNSTs derived from plexiform neurofibromas, 1488 and 96.2, expressed ASS1. This is unusual, as loss of ASS1, rather than gain, is often associated with tumorigenesis, as ASS1 is a known tumor suppressor.[29] It is possible that since plexiform neurofibromas are tumors, they have already lost ASS1 expression and during the mutation to MPNSTs, ASS1 could be reactivated for a variety of reasons. According to PhosphoSitePlus, a website dedicated to reporting information about post-translational modification, over 50 post-translational modification sites affecting ASS1 activity have been reported thus far.[30] To determine what is activating ASS1 in some cancers and not others, a proteomic analysis comparing ASS1 positive and negative cells would be necessary. It is also possible that *in vivo*, these cells would not express ASS1, however during growth in cell culture they have mutated to begin expressing ASS1 again. This is supported by two of the three lines that expressed ASS1 showing a drastic decrease into loss of ASS1 after freeze/thaw cycles, indicating ASS1 expression may be unstable in these MPNSTs, as well as the lack of expression in iHSCs, which we except to express ASS1 as they are not tumors, indicating their ASS1 expression may have changed upon immortalization.

We next examined how ADI-PEG20 affected mTORC1 activation, and found that the effect of arginine deprivation on mTORC1 activation is not dependent on ASS1 expression. We examined expression and activation of mTORC1 with and without ADI-PEG20, and found that arginine deprivation increased mTORC1 activation and expression in some lines, while it decreased in others, with no relationship to ASS1 expression. Additionally, expression and activation did not appear to be related. These indicate that ADI-PEG20 may be having some outside effects beyond arginine deprivation, or that arginine deprivation may be impacting other pathways not dependent on ASS1. One possibility is that other amino acids compensate for the absence of arginine caused by ADI-PEG20 treatment. Multiple amino acids, such as methionine, cysteine, and glutamate, have also been shown to interact with the RAGulator that regulates mTORC1 activity.[31] Each line of MPNSTs may compensate differently to arginine deprivation, resulting in mixed mTORC1 activation. While we expect arginine deprivation to decrease mTORC1 activation, it was unexpected that activation increased in some lines. A previous study showed that inhibition of mTORC1 through rapamycin increased the levels of arginine in Jurkat cells.[32] It is possible that this signaling could work in reverse in some MPNSTs, where decreased arginine increases mTORC1 activation. Future studies on other effects of ADI-PEG20 and other pathways affected by arginine deprivation are needed to fully explore this phenomenon.

We saw that both active and inactive mTORC1 bound to HK-II, and that arginine deprivation affected this in a manner unrelated to ASS1 expression. However, the data did begin to show a pattern in which lines with increased mTORC1 activity upon arginine deprivation have decreased HK-II binding upon arginine deprivation (HSC, 96.2), and lines with decreased mTORC1 activity upon arginine deprivation have increased HK-II binding upon arginine deprivation (ST03, 26T), with 1488 being the exception. This pattern indicates that inactive mTORC1 may preferentially bind to HK-II in MPNSTs, compared to active mTORC1. We would expect ADI-PEG20 treatment to inhibit binding of active mTORC1 to HK-II, so the increased binding with ADI-PEG20 treatment is unexpected. Again, this could be attributed to the relationship between arginine and mTORC1 inhibition mentioned above.[32] Arginine deprivation also impacted binding of inactive mTORC1 and HK-II, decreasing it in all lines except ST03, which showed a very small increase. This implies that mTORC1 may be localizing before it's active, and arginine deprivation prevents this, or that mTORC1 and HK-II are usually co-localized in MPNSTs and utilize the same metabolic method seen in Lu *et al.*, explaining the near ubiquitous preference for OXPHOS (Figure 2). It also indicates that arginine deprivation may encourage separation of mTORC1 and HK-II, perhaps due to the association between ADI and CAMs that affect mitochondrial activity.[31]

Further exploring the interaction between mTORC1 and HK-II with arginine deprivation, we saw that active mTORC1 and HK-II were both localized outside the nucleus, agreeing with previous information indicating mTORC1 can be localized to the mitochondria or Golgi[10] and that HK-II can be localized to the mitochondria.[25] We saw low levels of co-localization between mTORC1 and HK-II without arginine deprivation. Co-localization between active mTORC1 and HK-II increased with short term treatment, but the effect disappeared after longer treatment. While no studies have been performed showing the relationship between mTORC1 and HK-II localization and arginine, the relationship between arginine and mTORC1 activity mentioned above could offer a possible explanation.[32] This indicates that short term arginine deprivation may increase the interaction between mTORC1 and HK-II, while long term deprivation may either dampen mTORC1 and HK-II interaction, or lose its effect and return localization to that of the basal state. Losing the effect of arginine deprivation may be due to cells developing resistance to ADI-PEG20. Some cell lines developed resistance to ADI-PEG20 induced autophagy[19], and one method of this resistance may be reworking the metabolism to return mTORC1 and HK-II to their basal states. These data were only collected from HSCs and one line of MPNSTs (MP642), so it is difficult to generalize this reaction to arginine deprivation. This experiment should be repeated on multiple cell lines to see if the pattern repeats. Future studies should determine which organelle mTORC1 and HK-II co-localize to, as well as explore further the kinetics of arginine deprivation on mTORC1 localization.

A previous study had shown that co-localization of mTORC1 and HK-II at the mitochondria in irradiated cervical cancers and gliomas correlated to a shift from a glycolytic to OXPHOS metabolism[28], so we were interested to see if the co-localization of mTORC1 and HK-II we saw in MPNSTs corresponded to an OXPHOS phenotype (Figure 2). We observed a strong preference for OXPHOS metabolism in MPNSTs and their precursors, a surprise since many cancers favor a glycolytic phenotype. We believe this may be related to MPNST's location and origin. Schwann cells make up the myelin sheath, and exist in an extremely lipid rich environment, making OXPHOS more easily utilizable than glycolysis. While Seahorse analysis showed MPSNTs definitively favored OXPHOS, Western blots testing the expression of P-LDH and P-PDH, indicators of glycolysis, showed a range of expression from none to the same as positive controls. However, this does not mean that those lines showing high expression favored glycolysis. As shown by the Seahorse data, each line still performed some glycolysis, while favoring OXPHOS. The expression of P-LDH and P-PDH is perhaps just an indicator that these lines are also performing glycolysis, albeit at different levels. A piece of data that has potential clinical significance showed that HSCs had the ability to energetically compensate with glycolysis if OXHPOS was inhibited, while MPNSTs were not. This indicates that targeting the

OXPHOS metabolism in MPNSTs may be an effective strategy in stopping cellular growth or inducing apoptosis. Future studies should explore how ADI-PEG20 treatment affects metabolism. Previous studies exploring ADI-PEG20 showed in inhibited glycolysis, so it may not effect these OXPHOS favoring MPNSTs[19], however it is important to explore.

While very preliminary, these data show that arginine deprivation impacts the activation and localization of mTORC1, however this is not dependent on ASS1 expression. Additionally, we found that MPNSTs favor an OXPHOS phenotype, which may be related to the co-localization of mTORC1 and HK-II, and has potential clinical significance. However, most of the data shown came from only one repeat, so all experiments need to be repeated to obtain statistically significant results. In the future, I would like to explore if ADI-PEG20 affects survival of MPNSTs to determine if the any of the mixed effects of arginine deprivation on mTORC1 caused serious damage to the tumors. Previous studies have shown that ADI-PEG20 inhibits growth of sarcomas, so it is likely it would have the same effect on MPNSTs.[19] I would also inhibit mTORC1 and HK-II interaction using rapamycin, and determine if that causes a shift to aerobic glycolysis as predicted. If we did confirm that the OXPHOS phenotype was caused by mTORC1 binding to HK-II at the mitochondrial membrane, the next step would be finding a way to exploit that mechanism for treatment purposes. Exploring the mechanism behind metabolism provides important information that helps in targeting metabolism, providing a potentially successful treatment for an aggressive cancer like MPNSTs.

Methods

Reagents

Antibodies targeting phosphorylated (P) Raptor (Ser792), Raptor, phosphorylated lactate dehydrogenase A (P-LDHA) (Tyr10), LDHA, phosphorylated pyruvate dehydrogenase (P-PDH) (C54G1), PDH, phosphorylated pyruvate kinase M2 (P-PKM2) (Tyr105), and PKM2 were obtained from Cell Signaling Technologies. Anti-hexokinase II was obtained from Santa Cruz

Biotechnologies. Anti-β-actin and 4',6-diamidino-2-phenylindole (DAPI) were obtained from Sigma Aldrich. HRP-conjugated polyclonal goat anti-mouse, HRP-conjugated polyclonal goat anti-rabbit, and anti-argininosuccinate synthetase 1 (ASS1) were obtained from Abcam. Alexa Fluor 568 anti-mouse and FITC anti-goat were obtained from ThermoFisher. The argine deprivation agent, ADI-PEG20, was obtained from Polaris pharmaceuticals. Vectashield mounting medium was obtained from Vector Laboratories Inc.

Cell Lines

Lines 26T, 1488, STO3, 724, 96.2, S462, and ST88 were obtained from human malignant peripheral nerve sheath tumor (MPNST) patients. 26T was provided by Dr. Steven Porcelli (Albert Einstein College of Medicine, Bronx, NY), 724 was provided by Dr. Jonathan Fletcher), S462 was provided by Dr. Lan Kluwe (University Hospital Eppendorf, Hamburg, Germany), ST88 was provided by Dr. Jonathan Fletcher (Brigham and Women's Hospital, Boston, MA). iHSC, 1488, STO3, and 96.2 were provided by Dr. Angela Hirbe (Washington University School of Medicine, St. Louis, MO). Lines 85.116, 95.6, 062A, and 05.5 were obtained from human plexiform neurofibroma patients and provided by Dr. David Guttman (Washington University School of Medicine, St. Louis, MO). MG63, MNNG, and SK-LMS-1 lines were obtained from human osteosarcoma and leiomyosarcoma patients, provided by the Dr. Brian Van Tine (Washington University School of Medicine, St. Louis, MO). HSC were obtained from ABM. All cell lines were grown in a 5% CO_2 humidified incubator at 37° C and cultured in complete DMEM (D6046 supplemented with 5% fetal bovine serum). 24 hours before harvest, media was switched to MEM (M2279 supplemented with 5% glucose, 2.5% glutamine and 5% FBS).

Seahorse Metabolic Analysis (modified from Kremer et al., 2017 paper)

Samples were plated in a 10-cm dish with or without 1 μg/mL of ADI-PEG20. After 48 hr, cells were collected, and 20,000 cells were plated per well in a 96-well Seahorse plate with normal or ADI-PEG20 pretreated medium. Assays were performed 18–24 hours after plating with a Seahorse XF96 analyzer. Oligomycin was used at 10 mM in OXPHOS tests. Oligomycin was used at 5 mM for glycolysis tests. Oxygen consumption rate (OCR) measurements from mitochondrial stress tests are normalized to basal respiration rate, and extracellular acidification rate (ECAR) measurements from glycolysis stress tests are normalized to non-glycolytic ECARs. % OCR coupled to ATP synthesis was obtained from oligomycin decrease in OCR. All materials were obtained from Aligent Technologies.

ADI-PEG20 Treatment

ADI-PEG20 was diluted to 1 µg/mL in MEM (M2279 supplemented with 5% glucose, 2.5% glutamine and 5% FBS). Cellular media was replaced with MEM containing ADI-PEG20 and placed in a 5% CO_2 humidified incubator at 37° C for 24 hours.

Western Blotting

Cell pellets were collected, lysed with RIPA buffer, sonicated and incubated on ice for 30 minutes. Samples were then centrifuged for 15 min, at 4°C and supernatants were collected. Protein concentration was determined using a Quick Start Bradford assay (Bio-Rad). 40 µg of protein lysate were added per sample, diluted in H_2O to 20 µL, and diluted further with 2X SDS-PAGE Sample Buffer. Samples were boiled at 100°C for 5 minutes and ran through an SDS-PAGE gel at 140 volts for one hour. Samples were transferred onto PVDF membranes. Membranes were blocked with 5% milk in 1X 5% PBS-Tween for 30 minutes at room temperature. Primary antibodies were diluted in 5% milk in 1X 5% PBS-Tween and incubated at 4°C overnight. Antibodies against P-Raptor and ASS1 were diluted at 1:1000, while P-LDHA, LDHA, P-PDH, PDH, P-PKM2, PKM2, and Raptor were diluted at 1:500. Membranes were washed three times in 1X PBS-Tween for 5 minutes. 10 mL of 5% PBS-Tween was added to each blot along with secondary antibodies at a concentration of 1:10,000 and incubated for 1 hour. Washing was repeated. SuperSignal West Dura Extended Duration Substrate Kit (ThermoScientific) was used for visualization on a digital machine. Densitometry was performed using ImageJ software (Schneider, 2012).

Co-Immunoprecipitation of Hexokinase II and mTORC1

Cells were grown for 48 hours and were either treated with 1 μg/mL of ADI-PEG20 or left untreated for 4 hours. Samples were harvested with trypsin, washed twice with phosphate buffered saline (PBS), and pelleted by centrifuging at 1000xg for 5 minutes. Samples were lysed using 2%3-((3-cholamidopropyl) dimethylammonio)-1-propanesulfonate (CHAPS) buffer. Protein concentration was quantified using a Quick Start Bradford assay (Bio-Rad) read on a spectrophotometer at 595 nm. 40 μg of protein was mixed with 1 μL of anti-hexokinase II and samples were agitated at 4 °C overnight. The lysate was then added to 50 μL of protein G magnetic beads (Invitrogen) and mixed for 10 minutes at 37°C. Beads were allowed to migrate using a magnetic stand and flow through was removed. Beads were washed six times using 500 μL PBS with 0.1% Tween. 60 μL of 0.2M glycine (pH 2.5) were added tubes and incubated for 2 minutes. Samples were eluted from the beads and transferred to a new tube. Sample was concentrated by spinning at 14,000 x g for 30 minutes and eluted by spinning into a new column at 1000 x g for 2 minutes. Levels of phosphorylated (P)-Raptor, total Raptor, and β-actin were determined using Western blots.

Immunofluorescence

Cells (50,000) were plated on four-well chamber slides, grown for 24 hours, and treated with 1 μg/mL of ADI-PEG20 for 24, 6, or 4 hours, or left untreated. After ADI-PEG20 treatment, samples washed twice with phosphate-buffered saline (PBS), permeabilized with 0.5% Triton X-

100 in PBS at room temperature for 5 min, and fixed with 3% paraformaldehyde in PBS at room temperature for 15 min. Paraformaldehyde was removed by washing five times with PBS for a total of 5 min in a Coplin jar. Samples were blocked with 50% normal goat serum in PBS at 37°C for one hour. The cells were then stained with 1:100 anti-P-Raptor and 1:100 hexokinase II in antibody-binding solution (3% BSA, 0.5% Triton X-100, PBS) at 37°C for one hour. Cells were then washed with PBS 3 times in a Coplin jar and reacted with secondary antibodies, 1:500 AlexaFlour 568 and 1:200 FITC, in binding solution at 37°C for one hour. Cells were washed as before and placed under coverslips with Vectashield mounting medium and 100 μL DAPI. Images were taken using a confocal microscope at 1000x maginification. Excitation/emission for DAPI was at 358⁄461 nm, 490/525 nm for FITC, and 578/603 nm for AlexaFluor 568.

<u>Acknowledgements</u>

I would like to thank Dr. Olivia Hatton for her wise advice and support as my advisor and mentor throughout my college career. I would also like to thank her and Dr. Sara Hanson for their expertise, insights, and helpful feedback in writing and editing this thesis. I would like to thank Dr. Brian Van Tine, Dr. Bethany Prudner, and the rest of the Van Tine lab for serving as outstanding mentors throughout the research process. Finally, I would like to thank the Amgen Foundation for their monetary support that allowed me to perform research at Washington University School of Medicine.

Supplementary Figures

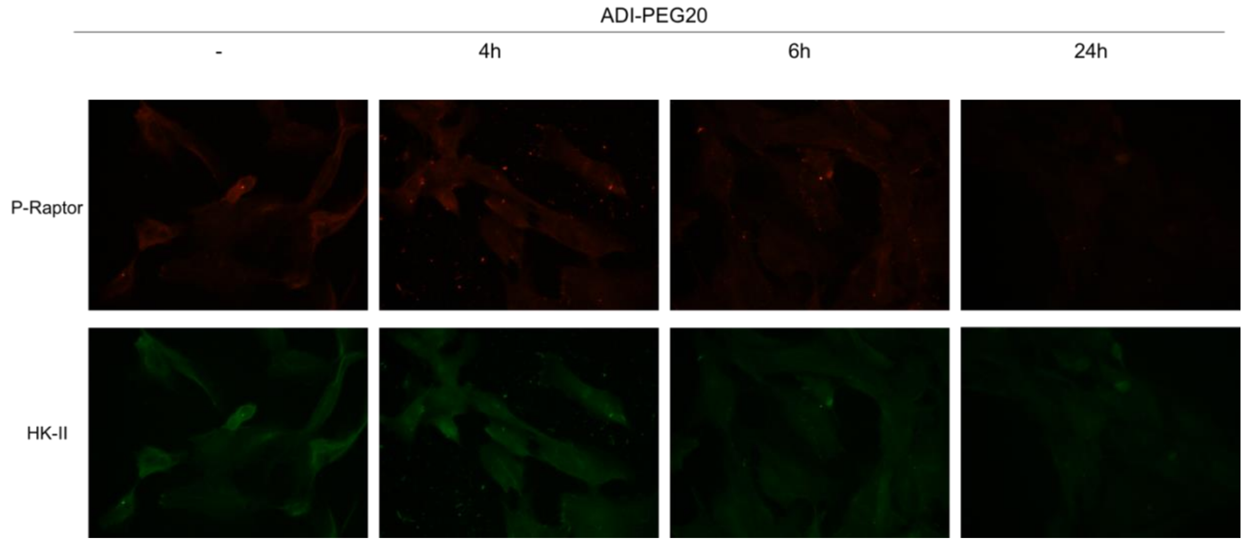

Supplemental Figure 1. mTORC1 and hexokinase II in Schwann cells (HSC). Schwann cells (HSC) were fixed and labeled after 1µg/mL of ADI-PEG20 treatment for 0, 4, 6, and 24 hours. Phosphorylated Raptor was labeled with AlexaFluor (red). Hexokinase II was labeled with FITC (green). This is representative of n=1 experiments.

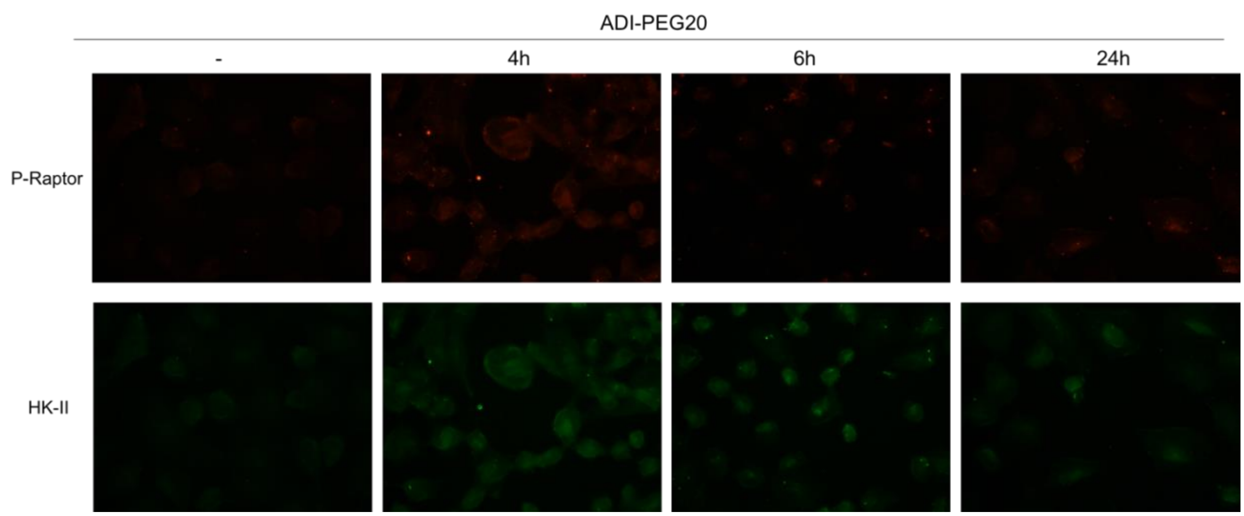

Supplemental Figure 2. mTORC1 and hexokinase II in MP642. MP642 cells were fixed and labeled after 1µg/mL of ADI-PEG20 treatment for 0, 4, 6, and 24 hours. Phosphorylated Raptor was labeled with AlexaFluor (red). Hexokinase II was labeled with FITC (green). This is representative of n=1 experiments.

References

1. Farid, M. *et al.* Malignant peripheral nerve sheath tumors. *Oncologist* **19**, 193-201 (2014).

2. Brekke, H.R. *et al.* Genomic changes in chromosomes 10, 16, and X in malignant peripheral nerve sheath tumors identify a high-risk patient group. *J Clin Oncol* **28**, 1573-1582 (2010).

3. Zhu, Y., Ghosh, P., Charnay, P. & Science, B.-D.K. Neurofibromas in NF1: Schwann cell origin and role of tumor environment. *Science* (2002).

4. Bradford, D. & Kim, A. Current treatment options for malignant peripheral nerve sheath tumors. *Curr Treat Options Oncol* **16**, 328 (2015).

5. Carli, M. *et al.* Pediatric malignant peripheral nerve sheath tumor: the Italian and German soft tissue sarcoma cooperative group. *J Clin Oncol* **23**, 8422-8430 (2005).

6. Saweyrs, C. Targeted cancer therapy. *Nature* **432**, 294-297 (2004).

7. Feun, L. *et al.* Arginine deprivation as a targeted therapy for cancer. *Current Pharmaceutical Design* **14**, 1049-1057 (2008).

8. Endo, M., Yamamoto, H., Setsu, N. & Cancer …, K.-K. Prognostic significance of AKT/mTOR and MAPK pathways and antitumor effect of mTOR inhibitor in NF1-related and sporadic malignant peripheral nerve …. *Clinical Cancer …* (2012).

9. Johansson, G. *et al.* Effective in vivo targeting of the mammalian target of rapamycin pathway in malignant peripheral nerve sheath tumors. *Mol Cancer Ther* **7**, 1237-1245 (2008).

10. Betz, C. & Hall, M.N. Where is mTOR and what is it doing there? *J Cell Biol* **203**, 563-574 (2013).

11. Holz, M.K., Ballif, B.A., Gygi, S.P. & Cell, B.-J. mTOR and S6K1 mediate assembly of the translation preinitiation complex through dynamic protein interchange and ordered phosphorylation events. *Cell* (2005).

12. Jewell, J.L., Russell, R.C. & Guan, K.-L. Amino acid signalling upstream of mTOR. *Nature reviews Molecular cell biology* **14**, 133-139 (2013).

13. Rebsamen, M., Pochini, L., Stasyk, T. & de Nature, M.E.G. SLC38A9 is a component of the lysosomal amino acid sensing machinery that controls mTORC1. *Nature* (2015).

14. Chantranupong, L. *et al.* The CASTOR Proteins Are Arginine Sensors for the mTORC1 Pathway. *Cell* **165**, 153-164 (2016).

15. Martina, J.A. & Biol, P.-R.J. Rag GTPases mediate amino acid–dependent recruitment of TFEB and MITF to lysosomes. *J Cell Biol* (2013).

16. Guoyao, W.U. & Journal, M.-S.M. Arginine metabolism: nitric oxide and beyond. *Biochemical Journal* (1998).

17. Wheatley, D.N., Philip, R. & Campbell, E. Arginine deprivation and tumour cell death: arginase and its inhibition. *Mol Cell Biochem* **244**, 177-185 (2003).

18. Wu, G. *et al.* Arginine metabolism and nutrition in growth, health and disease. *Amino Acids* **37**, 153-168 (2009).

19. Bean, G.R. *et al.* A metabolic synthetic lethal strategy with arginine deprivation and chloroquine leads to cell death in ASS1-deficient sarcomas. *Cell Death Dis* **7**, e2406 (2016).

20. Kremer, J.C. *et al.* Arginine Deprivation Inhibits the Warburg Effect and Upregulates Glutamine Anaplerosis and Serine Biosynthesis in ASS1-Deficient Cancers. *Cell Rep* **18**, 991-1004 (2017).

21. Cairns, R.A., Harris, I.S. & Mak, T.W. Regulation of cancer cell metabolism. *Nat Rev Cancer* **11**, 85-95 (2011).

22. Frezza, C. & Gottlieb, E. Mitochondria in cancer: not just innocent bystanders. *Seminars in cancer biology* (2009).

23. Munoz-Pinedo, C., El Mjiyad, N. & Ricci, J.E. Cancer metabolism: current perspectives and future directions. *Cell Death Dis* **3**, e248 (2012).

24. Tran, Q., Lee, H., Park, J., Kim, S.H. & Park, J. Targeting Cancer Metabolism - Revisiting the Warburg Effects. *Toxicol Res* **32**, 177-193 (2016).

25. Roberts, D.J. & Differentiation, M.-S. Hexokinase II integrates energy metabolism and cellular protection: Akting on mitochondria and TORCing to autophagy. *Cell Death & Differentiation* (2015).

26. Mathupala, S.P., Ko, Y.H. & in cancer biology, P.-P.L. Hexokinase-2 bound to mitochondria: cancer's stygian link to the "Warburg Effect" and a pivotal target for effective therapy. *Seminars in cancer biology* (2009).

27. Bustamante, E. & of the National, P.-P.L. High aerobic glycolysis of rat hepatoma cells in culture: role of mitochondrial hexokinase. *Proceedings of the National …* (1977).

28. Lu, C.L. *et al.* Tumor cells switch to mitochondrial oxidative phosphorylation under radiation via mTOR-mediated hexokinase II inhibition--a Warburg-reversing effect. *PLoS One* **10**, e0121046 (2015).

29. Miyamoto, T. *et al.* Argininosuccinate synthase 1 is an intrinsic Akt repressor transactivated by p53. *Science Advances* **3** (2017).

30. Hornbeck, P.V., Tkachev, S., Zhang, B. Skrzypek, E., Murray, B., Latham, V., Sullivan, M. PhosphoSitePlus: A comprehensive resource for investigation the structure and function of experimentally determined post-translational modifications in man and mouse. *Nucleic Acids Res.* **40**, D261-D270 (2012).

31. Nicastro, R., Sardu, A., Panchaud, N., De Virgilio, C. The Architecture of the Rag GTPase Signaling Network. *Biomolecules*. **7**, 48 (2017).

32. Ramanathan, A. and Schreiber, S.L. Direct Control of Mitochondrial Function by mTOR. *PNAS.* **106**, 22229-22232 (2009).